

A study of the centrally produced $\pi^+\pi^-\pi^0$ channel in pp interactions at 450 GeV/c

The WA102 Collaboration

D. Barberis⁵, W. Beusch⁵, F.G. Binon⁷, A.M. Blick⁶, F.E. Close⁴, K.M. Danielsen¹², A.V. Dolgoplov⁶, S.V. Donskov⁶, B.C. Earl⁴, D. Evans⁴, B.R. French⁵, T. Hino¹³, S. Inaba⁹, A.V. Inyakin⁶, T. Ishida⁹, A. Jacholkowski⁵, T. Jacobsen¹², G.V. Khaustov⁶, T. Kinashi¹¹, J.B. Kinson⁴, A. Kirk⁴, W. Klempt⁵, V. Kolosov⁶, A.A. Kondashov⁶, A.A. Lednev⁶, V. Lenti⁵, S. Maljukov⁸, P. Martinengo⁵, I. Minashvili⁸, K. Myklebost³, T. Nakagawa¹³, K.L. Norman⁴, J.M. Olsen³, J.P. Peigneux¹, S.A. Polovnikov⁶, V.A. Polyakov⁶, Yu.D. Prokoshkin^{†6}, V. Romanovsky⁸, H. Rotscheidt⁵, V. Rumyantsev⁸, N. Russakovich⁸, V.D. Samoylenko⁶, A. Semenov⁸, M. Sené⁵, R. Sené⁵, P.M. Shagin⁶, H. Shimizu¹⁴, A.V. Singovsky⁶, A. Sobol⁶, A. Solovjev⁸, M. Stassinaki², J.P. Stroot⁷, V.P. Sugonyaev⁶, K. Takamatsu¹⁰, G. Tchatchidze⁸, T. Tsuru⁹, G. Vassiliadis^{†2}, M. Venables⁴, O. Villalobos Baillie⁴, M.F. Votruba⁴, Y. Yasu⁹.

Abstract

The reaction $pp \rightarrow p_f(\pi^+\pi^-\pi^0)p_s$ has been studied at 450 GeV/c in an experiment designed to search for gluonic states. A spin analysis has been performed and the dP_T filter applied. The analysis confirms the previous observation that all undisputed $q\bar{q}$ states are suppressed at small dP_T . In addition, a clear difference is observed in the production mechanism for the η and ω .

Submitted to Physics Letters

† Deceased.

¹ LAPP-IN2P3, Annecy, France.

² Athens University, Nuclear Physics Department, Athens, Greece.

³ Bergen University, Bergen, Norway.

⁴ School of Physics and Astronomy, University of Birmingham, Birmingham, U.K.

⁵ CERN - European Organization for Nuclear Research, Geneva, Switzerland.

⁶ IHEP, Protvino, Russia.

⁷ IISN, Belgium.

⁸ JINR, Dubna, Russia.

⁹ High Energy Accelerator Research Organization (KEK), Tsukuba, Ibaraki 305, Japan.

- ¹⁰ Faculty of Engineering, Miyazaki University, Miyazaki, Japan.
- ¹¹ RCNP, Osaka University, Osaka, Japan.
- ¹² Oslo University, Oslo, Norway.
- ¹³ Faculty of Science, Tohoku University, Aoba-ku, Sendai 980, Japan.
- ¹⁴ Faculty of Science, Yamagata University, Yamagata 990, Japan.

The WA102 collaboration has recently described the application of a kinematical filter on centrally produced events [1]. This filter, which has been proposed as a glueball- $q\bar{q}$ filter [2], was originally based on the idea of Double Pomeron Exchange (DPE) and hence it is interesting to observe the effect of this filter on channels that cannot be produced by DPE. This paper presents new results from the WA102 experiment on the centrally produced $\pi^+\pi^-\pi^0$ final state in the reaction

$$pp \rightarrow p_f(\pi^+\pi^-\pi^0)p_s \quad (1)$$

at 450 GeV/c. The subscripts f and s indicate the fastest and slowest particles in the laboratory respectively. Due to the G parity of the $\pi^+\pi^-\pi^0$ system it cannot be produced by DPE. These data represent an increase by a factor of fifty in the previously published WA76 results on the centrally produced $\pi^+\pi^-\pi^0$ final state [3].

The data come from experiment WA102 which has been performed using the CERN Omega Spectrometer. The layout of the Omega Spectrometer used in this run is similar to that described in ref. [4] with the replacement of the OLGA calorimeter by GAMS 4000 [5].

Reaction (1) has been isolated from the sample of events having four outgoing charged tracks plus two γ s reconstructed in the electromagnetic calorimeter¹ by first imposing the following cuts on the components of the missing momentum: $|\text{missing } P_x| < 17.0 \text{ GeV}/c$, $|\text{missing } P_y| < 0.16 \text{ GeV}/c$ and $|\text{missing } P_z| < 0.12 \text{ GeV}/c$, where the x axis is along the beam direction. A correlation between pulse-height and momentum obtained from a system of scintillation counters was used to ensure that the slow particle was a proton.

The effective mass of the two γ s shows a clear π^0 signal ($\sigma = 17 \text{ MeV}$), which was selected by requiring $0.1 < m(\gamma\gamma) < 0.17 \text{ GeV}$. The quantity Δ , defined as $\Delta = MM^2(p_f p_s) - M^2(\pi^+\pi^-\pi^0)$, where $MM^2(p_f p_s)$ is the missing mass squared of the two outgoing protons, was then calculated for each event and a cut of $|\Delta| \leq 3.0 \text{ (GeV)}^2$ was used to select the $\pi^+\pi^-\pi^0$ channel. Events containing a fast $\Delta^{++}(1232)$ were removed if $M(p_f \pi^+) < 1.3 \text{ GeV}$, which left 1 323 136 centrally produced $\pi^+\pi^-\pi^0$ events. After the selection of the $\pi^+\pi^-\pi^0$ channel a kinematical fit was performed in order to apply overall energy and momentum balance.

Fig. 1a) shows the acceptance corrected $\pi^+\pi^-\pi^0$ effective mass spectrum renormalised to the total number of observed events. In addition to clear $\eta(547)$ and $\omega(782)$ signals there is a broad enhancement at 1.2 GeV, some evidence for the $a_2(1320)$ and another broad enhancement at 1.67 GeV.

A Dalitz plot analysis of the $\pi^+\pi^-\pi^0$ final state has been performed using Zemach tensors and a standard isobar model [6]. The analysis has assumed $\rho(770)$, σ , $f_0(980)$ and $f_2(1270)$ intermediate states and that only relative angular momenta up to 2 contribute. For the $\rho\pi$ decays both $I = 0$ and $I = 1$ final states have been considered. The σ stands for the $\pi\pi$ S-wave amplitude squared, and the parameterisation of Zou and Bugg [7] has been used in this analysis.

The geometrical acceptance of the apparatus has also been evaluated over the Dalitz plot of the $\pi^+\pi^-\pi^0$ system in 40 MeV intervals between 0.8 and 2.0 GeV. In order to perform a spin parity analysis the log likelihood function, $\mathcal{L}_j = \sum_i \log P_j(i)$, is defined by combining the

¹The showers associated with the impact of the charged tracks on the calorimeter have been removed from the event before the requirement of only two γ s was made.

probabilities of all events in 40 MeV $\pi^+\pi^-\pi^0$ mass bins from 0.84 to 2.0 GeV. In order to include more than one wave in the fit the incoherent sum of various event fractions a_j is calculated:

$$\mathcal{L} = \sum_i \log \left(\sum_j a_j P_j(i) + (1 - \sum_j a_j) \right) \quad (2)$$

where the term $(1 - \sum_j a_j)$ represents the phase space background which is a free parameter in each bin. The negative log likelihood function $(-\mathcal{L})$ is then minimised using MINUIT [8]. Coherence between different J^P states and between different isobar amplitudes of a given J^P have been neglected in the fit. Different combinations of waves and isobars have been tried and insignificant contributions have been removed from the final fit. Using Monte Carlo simulations it has been found that the feed-through from one spin parity to another is negligible and that the peaks in the spin analysis cannot be produced by phase space or acceptance effects. The fit generates the phase space background as that part of the data not associated with a given wave on a bin by bin basis and one requirement is that this background is a smoothly varying function that shows no residual resonance structure.

The result of the best fit is shown in fig. 2 for the total data sample. A fit using $J^{PC} = 1^{++} \rho^\pm \pi^\mp$ S-wave, $J^{PC} = 2^{++} \rho^\pm \pi^\mp$ D-wave, $J^{PC} = 2^{-+} \rho^\pm \pi^\mp$ P-wave, $J^{PC} = 2^{-+} f_2(1270)\pi^0$ S-wave, $J^{PC} = 1^{--} \rho\pi$ P-wave and phase space is found to be sufficient in order to describe the data. The phase space distribution resulting from the fit shows no remaining resonance structure.

The $J^{PC} = 1^{++} \rho^\pm \pi^\mp$ S-wave shows a broad enhancement. It has been fitted using an expression of the form:

$$\frac{dN}{dm} = \frac{m_{a_1} \Gamma_{a_1}(m)}{(m^2 - m_{a_1}^2)^2 + \Gamma_{a_1}^2(m) m_{a_1}^2} \quad (3)$$

where $\Gamma_{a_1}(m)$ is a mass dependent width of the form

$$\Gamma_{a_1}(m) = \Gamma_{a_1} m_{a_1} \frac{\rho^{1+S}(m)}{\rho^{1+S}(m_{a_1})} \quad (4)$$

where $\rho^{1+S}(m)$ is the phase space for S-wave $\rho^\pm(770)\pi^\mp$, including the effects of the mass dependent $\rho^\pm(770)$ width and of interference between the two $\rho^\pm(770)$ bands in the Dalitz plot [9]. The results of the fit are given in table 1 and the mass and width are consistent with the PDG values for the $a_1(1260)$ [10].

The $J^{PC} = 2^{++} \rho^\pm \pi^\mp$ D-wave shows a peak in the $a_2(1320)$ region and has been fitted using a relativistic spin 2 Breit-Wigner. The results of the fit are given in table 1. The $J^{PC} = 2^{-+} \rho^\pm \pi^\mp$ P-wave and $J^{PC} = 2^{-+} f_2(1270)\pi^0$ S-wave have similar distributions consistent with the $\pi_2(1670)$. The $J^{PC} = 2^{-+} \rho^\pm \pi^\mp$ P-wave has been fitted with a spin 1 relativistic Breit-Wigner and the $J^{PC} = 2^{-+} f_2(1270)\pi^0$ S-wave has been fitted with a spin 0 relativistic Breit-Wigner. The masses and widths are similar and are given in table 1. The $J^{PC} = 1^{--} \rho^\pm \pi^\mp$ P-wave is dominated by a peak at the mass of the $\phi(1020)$ which has been fitted with a spin 1 relativistic Breit-Wigner convoluted with a Gaussian to describe the experimental resolution.

The $\pi^+\pi^-\pi^0$ mass spectrum shown in fig. 1a) has been fitted with the resonances described above together with a Gaussian ($\sigma = 11\text{MeV}$) to describe the η , a Breit-Wigner convoluted with

a Gaussian ($\sigma = 18$ MeV) to describe the ω and a background of the form $a(m - m_{th})^b \exp(-cm - dm^2 - em^3)$, where m is the $\pi^+\pi^-\pi^0$ mass, m_{th} is the threshold mass and a,b,c,d,e are fit parameters. The fit is found to describe the data well and yields masses for the η and ω given in table 1.

The branching ratio for the $\pi_2(1670)$ to $\rho\pi$ and $f_2(1270)\pi$ has been calculated taking into account the unseen decay modes of the $f_2(1270)$ and gives

$$\frac{\pi_2(1670) \rightarrow \rho\pi}{\pi_2(1670) \rightarrow f_2(1270)\pi} = 0.57 \pm 0.02_{-0.02}^{+0.03} \quad (5)$$

which is in good agreement with the PDG values of 0.55 ± 0.08 [10]. The systematic error quoted has three major sources. The first comes from the error in the branching ratio of $f_2(1270)$ to $\pi\pi$ [10]. The second is due to the determination of the number of events in each decay mode; this has been estimated by comparing the ratio calculated from the total data sample compared to the ratio calculated from the fits performed as a function of dP_T (see below). Finally estimates of possible backgrounds below the signals have been made for both decay modes.

In previous analyses of other channels it has been observed that when the centrally produced system has been analysed as a function of the parameter dP_T , which is the difference in the transverse momentum vectors of the two exchange particles [1], all the undisputed $q\bar{q}$ states are suppressed at small dP_T . Therefore a study of the $\pi^+\pi^-\pi^0$ system has been made as a function of dP_T . The $\pi^+\pi^-\pi^0$ mass spectrum is presented in fig. 1b), c) and d) for $dP_T \leq 0.2$ GeV, $0.2 \leq dP_T \leq 0.5$ GeV and $dP_T \geq 0.5$ GeV respectively. In order to determine the dependence of the η and the ω as a function of dP_T , a fit has been made to these mass spectra using the parameters from the fit to the total mass spectrum. For the $a_1(1260)$, $a_2(1320)$, $\pi_2(1670)$ and $\phi(1020)$ the spin analysis has been performed as a function of dP_T and the results are shown in fig. 3. The $J^{PC} = 2^{-+} \rho^\pm\pi^\mp$ P-wave and $J^{PC} = 2^{-+} f_2(1270)\pi^0$ S-wave have been summed together to produce a single $J^{PC} = 2^{-+}$ wave. The waves have been fitted with the Breit-Wigners described above and the results are given in table 2. As can be seen all the resonances are suppressed at small dP_T . However, it is interesting to note that they do not all have the same dP_T behaviour.

The azimuthal angle (ϕ) between the fast and slow proton is related to dP_T by

$$\cos\phi = \frac{P_T^2 - dP_T^2}{4P_{T1}P_{T2}}$$

where P_T is the transverse momentum of the central system and $P_{T1,2}$ is the transverse momentum of the exchanged particle. From table 2 it can be seen that the η and the ω have a similar dP_T dependence; however, they have a dramatically different ϕ dependence. Fig. 4a) and b) show the angle ϕ for $0.5 \leq m(\pi^+\pi^-\pi^0) \leq 0.6$ GeV (η region) and for $0.735 \leq m(\pi^+\pi^-\pi^0) \leq 0.835$ GeV (ω region) respectively. This suggests that the η and the ω have very different production mechanisms. Further evidence for this comes from studying the four momentum transfer squared from one of the proton vertices which is shown in fig. 4c) and d) for the η and ω respectively. The $|t|$ distribution for the ω is more steep than that for the η and extends to $|t| = 0$ unlike the η distribution which appears to turn over.

In order to investigate the centre of mass energy dependence of η and ω production, the ratio of the acceptance corrected number of η s and ω s has been calculated using data from the WA76

experiment which was performed at an incident beam energy of 85 GeV/c ($\sqrt{s} = 12.7$ GeV) [3] and from this current experiment ($\sqrt{s} = 29$ GeV).

$$\frac{\sigma(\eta)}{\sigma(\omega)} = 0.20 \pm 0.02 (\sqrt{s} = 12.7 \text{ GeV}) = 0.09 \pm 0.01 (\sqrt{s} = 29 \text{ GeV}) \quad (6)$$

which again indicates a different production mechanism for the two resonances.

In summary, a study of the centrally produced $\pi^+\pi^-\pi^0$ system shows that the most prominent resonance signals are due to the η , ω , $\phi(1020)$, $a_1(1260)$, $a_2(1320)$ and $\pi_2(1670)$. All these states are found to be suppressed at small dP_T . In addition, a clear difference is observed in the production characteristics of the η compared to the ω .

References

- [1] D. Barberis *et al.*, Phys. Lett. **B397** (1997) 339.
- [2] F.E. Close and A. Kirk, Phys. Lett. **B397** (1997) 333.
- [3] T.A. Armstrong *et al.*, Zeit. Phys. **C48** (1990) 213.
- [4] F. Antinori *et al.*, Il Nuovo Cimento **A107** (1994) 1857.
- [5] D. Alde *et al.*, Nucl. Phys. **B269** (1986) 485.
- [6] M. Abramovich *et al.*, Nucl. Phys. **B23** (1970) 466.
- [7] B. S. Zou and D. V. Bugg, Phys. ReV. **D48** (1993) R3948.
- [8] F. James and M. Roos, MINUIT Computer Physics Communications **10** (1975) 343; CERN-D506 (1989).
- [9] M.G. Bowler, Phys. Lett. **B182** (1986) 400.
- [10] Particle Data Group, Phys Rev. **D54** (1996) 1.

Tables

Table 1: Parameters of resonances in the fit to the $\pi^+\pi^-\pi^0$ mass spectrum and waves.

	Mass (MeV)	Width (MeV)	Observed decay mode	$I(J^{PC})$	Number of events
η	549 ± 1	-		$0(0^{-+})$	21590 ± 644
$\omega(782)$	785 ± 2	8.4 (fixed)		$0(1^{--})$	248511 ± 2118
$\phi(1020)$	1021 ± 4	4 (fixed)	$\rho\pi$	$0(1^{--})$	9053 ± 490
$a_1(1260)$	1240 ± 10	400 ± 35	$\rho\pi$	$1(1^{++})$	327957 ± 2678
$a_2(1320)$	1317 ± 3	120 ± 10	$\rho\pi$	$1(2^{++})$	35616 ± 648
$\pi_2(1670)$	1669 ± 4 1670 ± 4	268 ± 15 256 ± 15	$\rho\pi$ $f_2(1270)\pi$	$1(2^{-+})$ $1(2^{-+})$	23535 ± 598 23692 ± 549

Table 2: Resonance production as a function of dP_T expressed as a percentage of its total contribution.

	$dP_T \leq 0.2$ GeV	$0.2 \leq dP_T \leq 0.5$ GeV	$dP_T \geq 0.5$ GeV
η	$5.3 \pm 0.5 \pm 0.5$	$42 \pm 1 \pm 1$	$52 \pm 1 \pm 1$
$\omega(782)$	$13 \pm 1 \pm 1$	$44 \pm 1 \pm 1$	$43 \pm 1 \pm 1$
$\phi(1020)$	$8 \pm 2 \pm 2$	$47 \pm 3 \pm 3$	$45 \pm 2 \pm 4$
$a_1(1260)$	$17 \pm 1 \pm 3$	$53 \pm 3 \pm 2$	$29 \pm 2 \pm 2$
$a_2(1320)$	$4 \pm 2 \pm 3$	$37 \pm 2 \pm 1$	$59 \pm 3 \pm 3$
$\pi_2(1670)$	$15 \pm 1 \pm 1$	$51 \pm 2 \pm 3$	$33 \pm 1 \pm 3$

Figures

Figure 1: The $\pi^+\pi^-\pi^0$ effective mass spectrum a) for the total data with fit using 3 Breit-Wigners b) for $dP_T \leq 0.2$ GeV, c) for $0.2 \leq dP_T \leq 0.5$ GeV and d) for $dP_T \geq 0.5$ GeV.

Figure 2: Results of the spin parity analysis. The superimposed curves are the resonance contributions coming from the fits described in the text.

Figure 3: Results of the spin parity analysis as a function of dP_T .

Figure 4: The azimuthal angle (ϕ) between the two outgoing protons for the a) η and b) ω . The four momentum transfer squared ($|t|$) from one of the proton vertices for the c) η and d) ω .

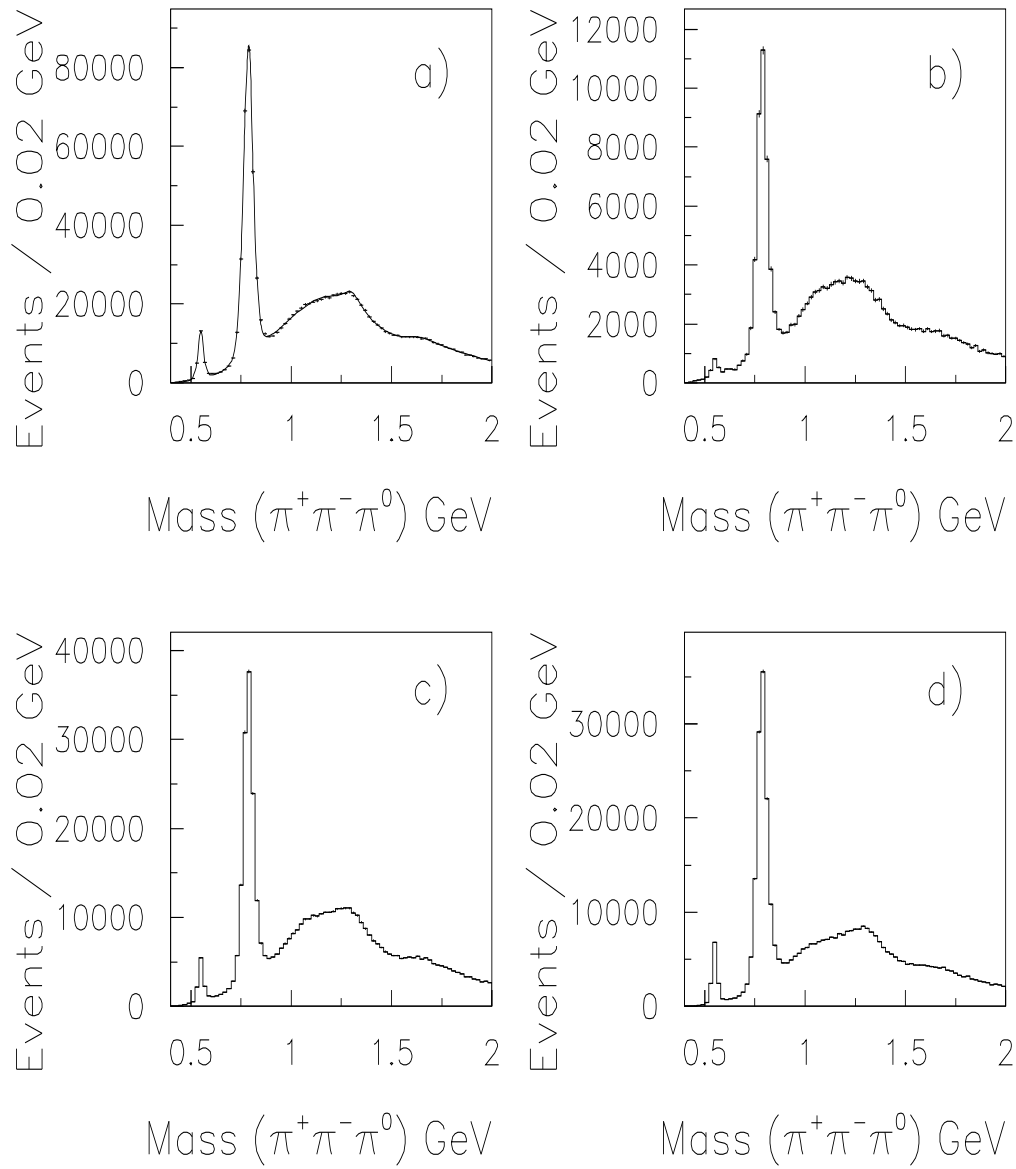


Figure 1

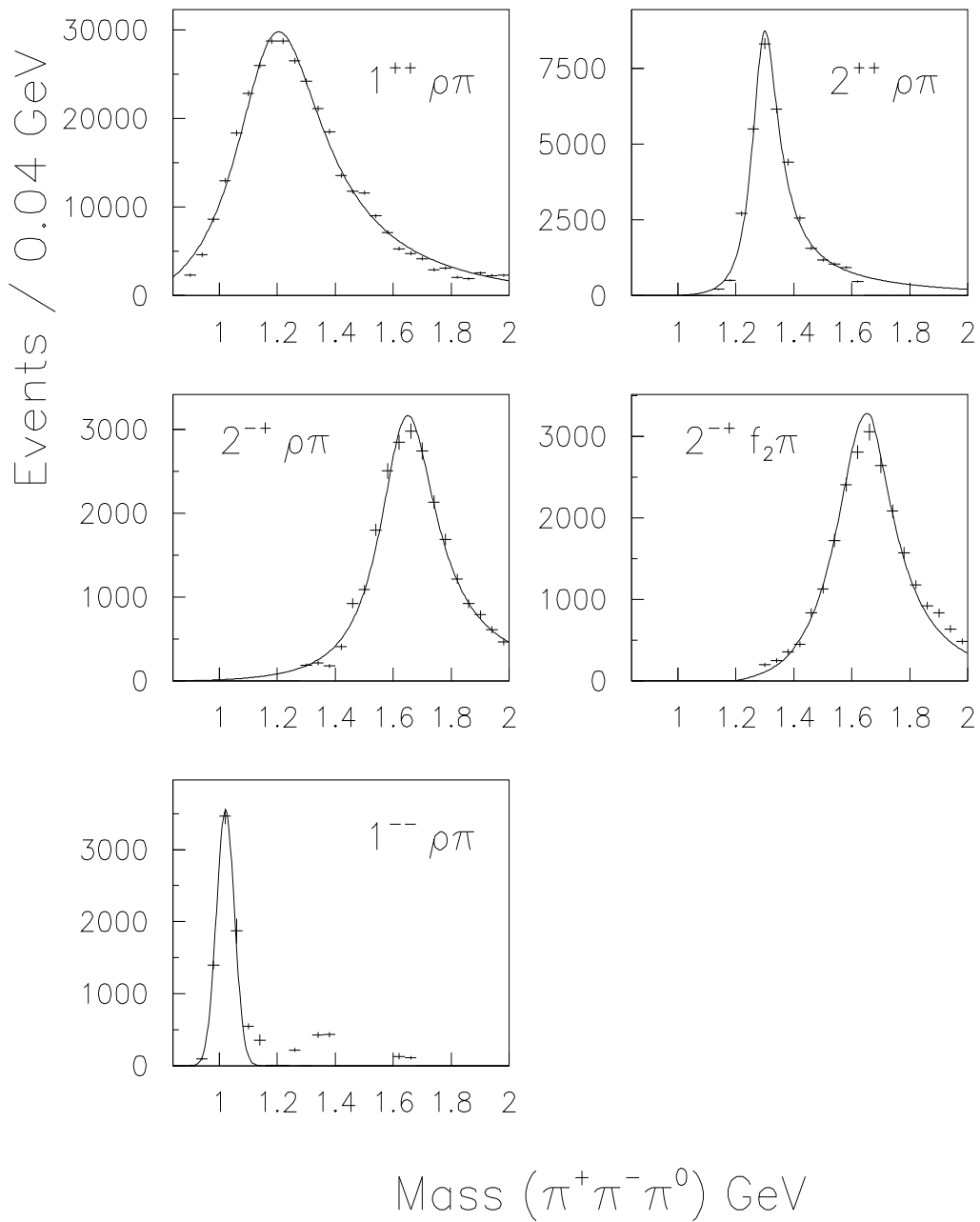


Figure 2

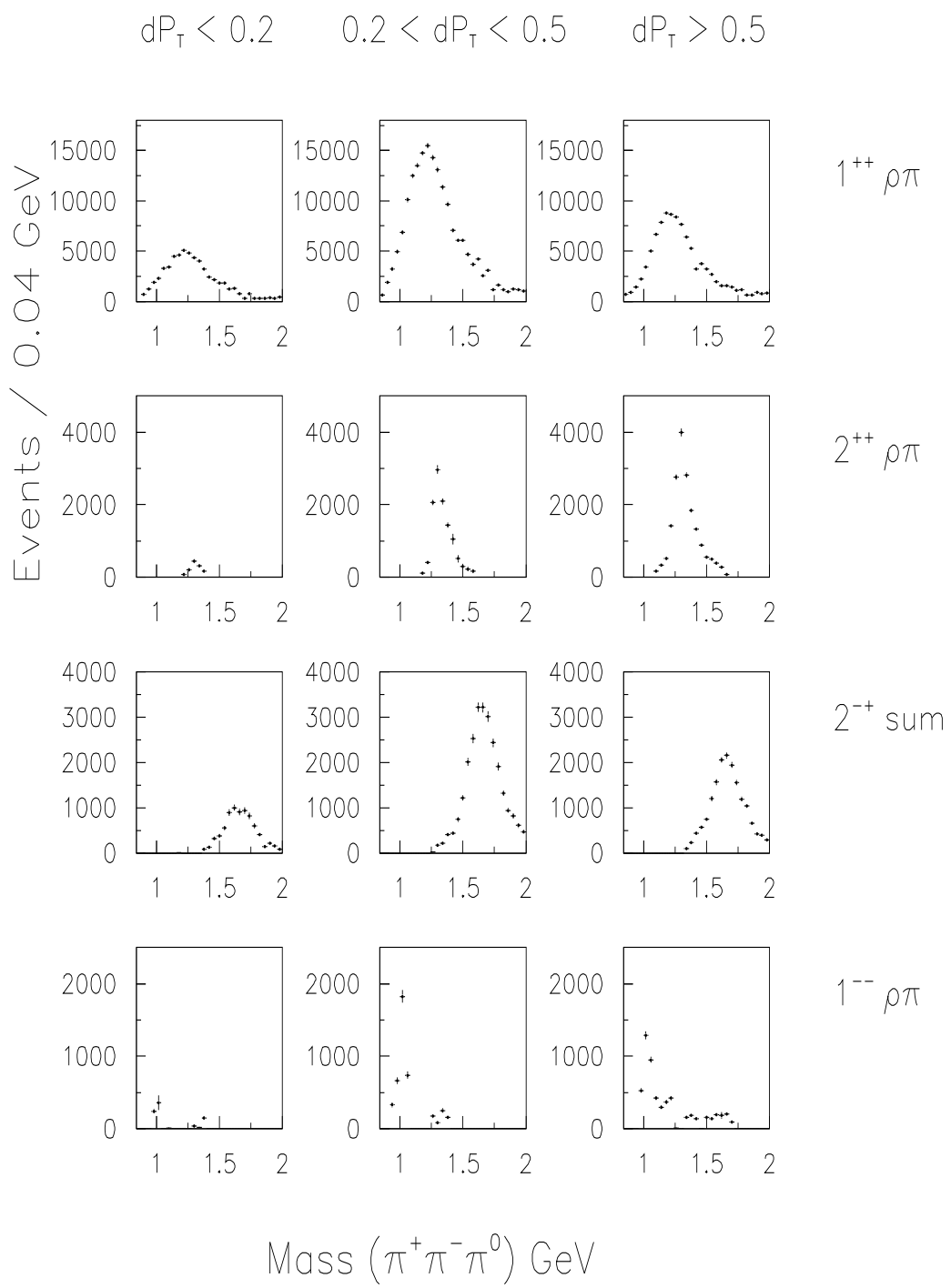


Figure 3

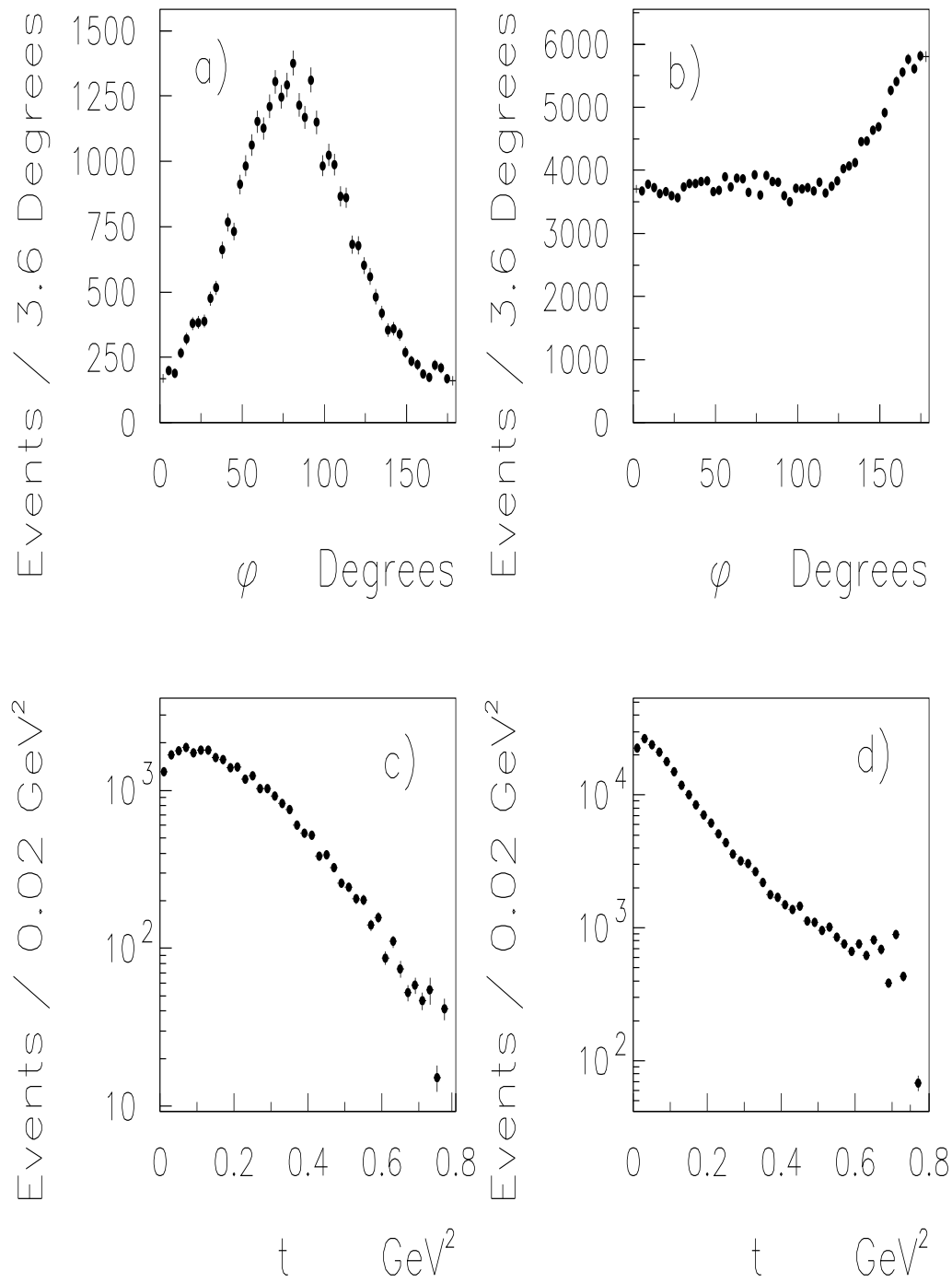


Figure 4